Perfluoropolyethers: Analysis by TOF-SIMS

A. M. Spool*

IBM Storage Systems Division, San Jose, California 95193

Paul H. Kasai*

IBM Research Division, Almaden Research Center, San Jose, California 95120

Received September 7, 1995[⊗]

ABSTRACT: TOF-SIMS spectra of the following perfluoropolyethers (PFPEs) were analyzed: Demnum-S, Krytox, Fomblin-Z, perfluoropoly(dioxolane), perfluoropoly(tetramethylene oxide), and perfluoropoly(ethylene oxide). In each case, the PFPE produced an intense negative ion spectrum with simple patterns persisting into the high-mass region surpassing the mean MW of the polymer. In contrast, the positive ion spectra are much more complex and compressed toward the low-mass end. Totally unrelated formation mechanisms for the positive and negative ions are thus indicated. It is proposed and substantiated that the negative ion spectra are dominated by anions resulting from one-step dissociative electron capture at ether oxygens, $R-O-R' + e^- \rightarrow R-O^- + {}^\bullet R'$. The Demnum molecule, having locally symmetric ether oxygens, produces two major peaks in each repetitive fragmentation packet, equal in intensity but displaced by the mass difference of the two end groups. PFPEs with asymmetric ether oxygens produce negative ion spectra resulting from asymmetric cleavage. The negative ion pattern of Fomblin-Z can be accurately modeled with the dissociative electron capture at ether oxygens linking randomly distributed methylene and ethylene units. Other less intense peaks in the negative ion spectra of PFPEs result from multiple electron capture events and from polymer chains with anomalous end groups or intrachain units.

Introduction

Perfluoropolyethers (PFPEs) are currently the lubricant of choice for magnetic recording media[1] and are also in use as lubricants in such severe environments as aerospace engines and satellite instruments.[2] These polymers have a wide liquid-phase temperature range (−100 to +400 °C). ^{19}F NMR spectroscopy thus has proven to be extremely efficacious for analysis of PFPEs available in quantity.[3] Analysis of PFPEs present on solid surfaces as lubricants is a task of greater challenge. To this end, significant success in the understanding of surface-bound PFPEs has been obtained using static secondary ion mass spectrometry (SSIMS).[4−13] In particular, SSIMS has been used to quantify thin (<3 nm) PFPE layers[9,10] and to determine the average molecular weight (M_n) from the relative intensities of peaks in the fragmentation patterns.[11] It has also been shown that the molecular weight distribution of PFPEs may be determined by time-of-flight secondary ion mass spectrometry (TOF-SIMS). The distribution analysis is made possible by the high mass range of TOF-SIMS and "cationization" of parent PFPE chains when desorbed from a certain metal surface.[7,8,11] Finally, different end groups have been detected and identified with the aid of TOF-SIMS.[8,11]

Examination of reported TOF-SIMS spectra of PFPEs and those of our own revealed immediately that, while the negative ion spectra have intense but simple patterns persisting into the high-mass region surpassing the mean MW of the polymers, the positive ion spectra are much more complex and compressed toward the low-mass end. Totally unrelated formation/decay mechanisms for the positive and negative ions are thus indicated.

It is well known that when a beam of high-energy X-rays, electrons, or positive ions traverses through a material, essentially all of the energy dissipation (of the primary beam) occurs through ionization of media molecules, and "chemical events" are caused by numerous secondary electrons generated through cascading processes. This common mechanism explains why the relative sensitivities of various polymer materials to X-rays, ion beams, and electron beams are the same.[14] It is also well known that large organic molecules, upon impact with high-energy electrons, undergo (multiple) fragmentation and generate series of positively charged fragments weighted toward the low-mass end.[15] The positive ion spectra of TOF-SIMS of PFPEs may hence be attributed to fragmentation processes caused by energetic secondary electrons.

For the negative ion formation, the most plausible mechanisms are (1) ion-pair formation, heterolytic cleavage of excited neutral fragments (or molecules), $A-B^* \rightarrow A^+ + B^-$, and (2) dissociative electron capture, capture of secondary electrons of thermal energy (insufficient for further ionization) by molecules having electrophilic sectors, leading to a reaction of the form $A-X-B' + e^- \rightarrow A-X^- + {}^\bullet B$. The ion-pair formation requires the existence and occupation of unique excited state(s).[15] For many organic polymer molecules, electrophilic sectors are ubiquitous, and the cross section for dissociative electron capture by such segments is much larger than those for other fragmentation mechanisms. Typical G values (the number of chemical events induced for each 100 eV of energy absorbed from an electron beam) of ordinary polymers such as polyethylene, polystyrene, or poly(methyl methacrylate) are in the range of 0.1−1.0. These G values increase to ∼10 when polymer chains incorporate electrophilic groups as in poly(butene sulfone), or obtain electrophilic substituents as in epoxylated poly(methyl methacrylate)s.[14] It has been demonstrated that the increased sensitivities of these polymers are due to dissociative electron capture at the electrophilic sites.[16,17]

We propose that the prominent, persistent patterns uniquely observed in the negative ion TOF-SIMS spec-

[⊗] Abstract published in *Advance ACS Abstracts,* February 1, 1996.

0024-9297/96/2229-1691$12.00/0

Table 1. Formulae of Perfluoropolyethers Examined in the Present Study

Demnum	$CF_3-CF_2-CF_2-O-\left(CF_2-CF_2-CF_2-O\right)_m-CF_2-CF_3$
Krytox	$CF_3-CF_2-CF_2-O-\left(\underset{F}{\overset{CF_3}{\overset{\vert}{\underset{\vert}{C}}}}-CF_2-O\right)_m-CF_2-CF_3$
Fomblin Z	$CF_3-O-\left(CF_2-CF_2-O\right)_m-\left(CF_2-O\right)_n-CF_3$ (m/n = 4/5)
PFP(Dioxolane)	$CF_3-O-\left(CF_2-CF_2-O-CF_2-O\right)_m-CF_3$
PFP(Tetramethylene Oxide)	$CF_3-CF_2-CF_2-O-\left(CF_2-CF_2-CF_2-CF_2-O\right)_m-CF_2-CF_2-CF_3$
PFP(Ethylene Oxdie)	$CF_3-O-\left(CF_2-CF_2-O\right)_m-CF_3$

tra of PFPEs are due to negative ions produced by one-step dissociative electron capture at ether oxygens.

$$R-O-R' + e^- \rightarrow R-O^- + {}^{\bullet}R'$$

Reported below are results of TOF-SIMS study of six different PFPEs. The positive and negative ion spectra were compared, and the persistent patterns of negative ion spectra were analyzed in detail. It is revealed, for each PFPE, that all the major peaks in the persistent negative ion pattern are due to anions resulting from electron capture at ether oxygens.

Experimental Section

Table 1 gives the formula (the repeat units and most typical end groups) of the six PFPEs examined in the present study. Demnum-S, Krytox, and Fomblin-Z are commercial products of Daikin Ind. (of Japan), Du Pont (of USA), and Montefluos (of Italy), respectively. Perfluoropoly(dioxolane), perfluoropoly(tetramethylene oxide), and perfluoropoly(ethylene oxide) are experimental materials kindly supplied by the fluorochemical group of 3M (St. Paul, MN). The latter three are notated as PFP(dioxolane), PFP(tetramethylene oxide), and PFP(ethylene oxide), respectively, in the remaining report.

TOF-SIMS spectra were obtained from samples smeared onto Si wafers; thus all the analyses described are essentially of "bulk" materials. Previous works using both NMR and TOF-SIMS have noted the presence of impurities in these PFPEs with differing end groups. They are noted in the text where appropriate.

TOF-SIMS measurements were performed using a Charles Evans and Associates TRIFT spectrometer. This instrument has been described in detail elsewhere.[18,19] The primary ions used for most of this work were from a pulsed Cs^+ source operating at 11 keV. Secondary ion extraction was accomplished with a ±3 keV bias on the sample. One consequence of this extraction field is that the primary ion impact energy is 8 keV in positive ion mode and 14 keV in negative ion mode. Where comparisons were made between positive and negative ion yields, a pulsed liquid metal ion gun (Ga^+ source) operating at 25 keV was hence used. The smaller relative difference between the impact energies in positive (22 keV) and negative (28 keV) ion modes made intensity comparisons more direct. The spectra (used for yield comparison) were obtained after an extended warm-up of the source for several hours and were all taken within the next few hours and with the same pulse width (4 ns), repetition rate, and acquisition time. For all spectra obtained in this study, the total ion dose was kept below 10^{12} ions cm^{-2}, lower than the generally accepted static limit.[20]

Results and Discussion

Positive Ion vs Negative Ion Spectra. Cascading ionization/fragmentation processes initiated by the primary ion beam in TOF-SIMS experiment of PFPEs are depicted schematically in Figure 1. Positive ions are thus formed as the result of ionization by the primary ions and, much more often, by numerous energetic secondary electrons. Negative ions are formed via dissociative capture of low-energy secondary electrons. The most probable dissociative capture expected here is that yielding F^- ions, i.e., $R-F + e^- \rightarrow R^{\bullet} + F^-$. Negative ions responsible for the pattern extending into high-mass range are produced by dissociative electron capture at ether oxygens as discussed earlier. The positive ions are products of high-energy processes and are produced closer to the trajectory of the primary beam. A higher degree of fragmentation and lower stability are expected for these ions. The negative ions are products of a low-energy process and are more likely produced in the circumjacent region. A recent TOF-SIMS study of Krytox[13] has shown the short lifetimes of positive ions and the relative stability of negative ions in accord with the mechanism depicted here.

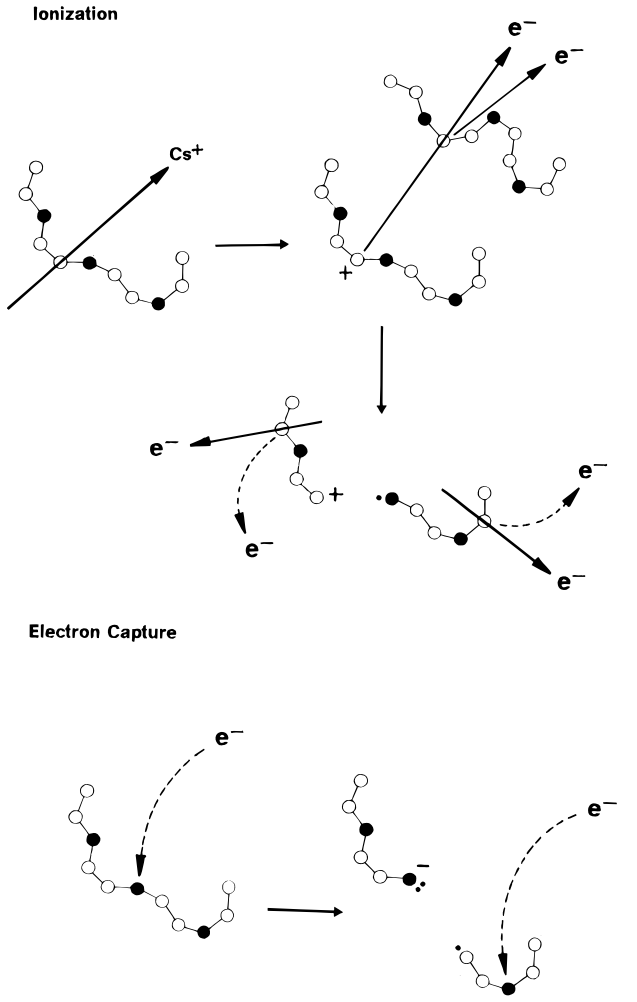

Figure 1. Schematic representation of SIMS experiment on perfluoropolyethers. Open and solid circles indicate CF_2 and ether oxygen, respectively. Positive ion fragments are produced via ionization by the primary beam (Cs^+ ions) and by energetic secondary electrons. Negative ions are produced on capture of low-energy secondary electrons.

Figure 2 shows the negative and positive ion TOF-SIMS spectra obtained from Demnum-S. The spectra, shown in the same logarithmic scale, were obtained with identical primary ion doses. The difference in the yield characteristics of the positive and negative ions is conspicuous. The negative ion yield above 200 amu is at least 2 orders of magnitude larger than the positive

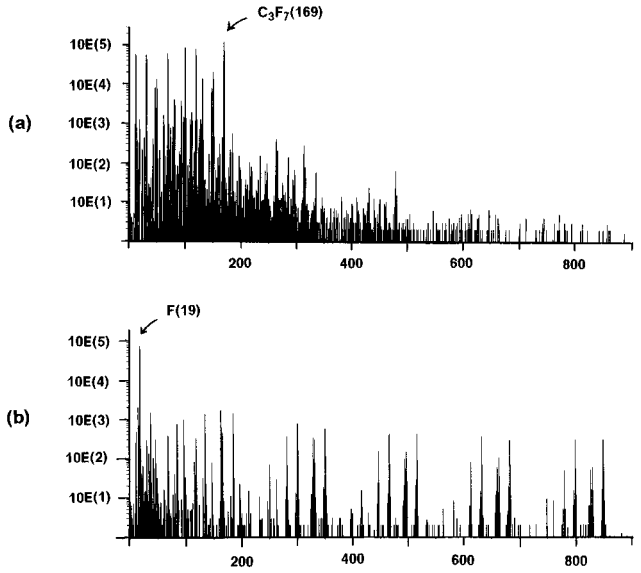

Figure 2. TOF-SIMS spectra of Demnum: (a) positive ion spectrum; (b) negative ion spectrum. The spectra, shown in the logarithmic scale, were obtained under the identical dosage condition.

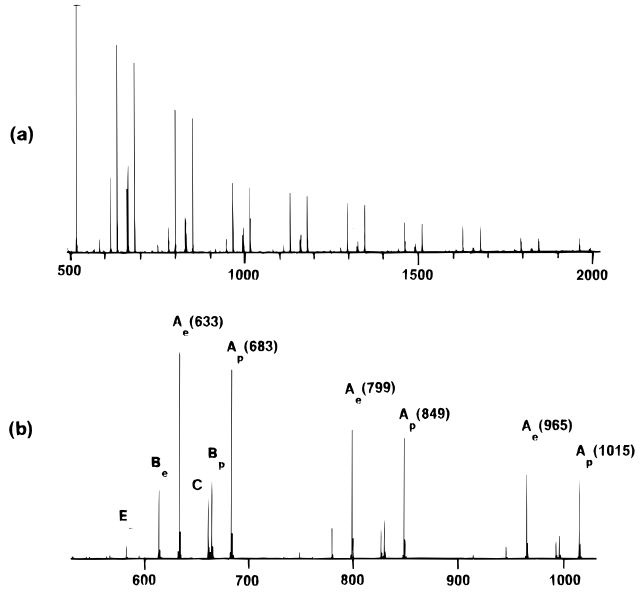

Figure 3. (a) Negative ion TOF-SIMS spectrum of Demnum shown in a linear scale for the 500−2000 amu range. (b) A section of (a) encompassing three successive repeat packets.

ion yield. In the positive ion spectrum, intense peaks are all under 200 amu and are attributable to fragments having three or fewer CF_2 units. Past 200 amu, a series of peaks are seen in an almost continuous fashion, but their intensities decrease rapidly with increasing mass. In the negative ion spectrum, the most intense peak is that of F^- as expected. The F^- peak (19 amu) is followed by a series of peaks of medium intensity which decreases gradually with increasing mass. The series continues into the high-mass range, surpassing the mean molecular weight of the polymer (>2000 amu).

Dissociative Electron Capture at Ether Oxygens. Demnum-S. Figure 3a shows, in a linear scale, the negative ion spectrum of Demnum-S in the 500−2000 amu range. Figure 3b shows, in an expanded scale, its portion encompassing three repetitive packets of the pattern. As expected, packets are separated by 166 amu, the mass of the monomer repeat unit, $CF_2CF_2CF_2O$. The two major peaks in each packet are

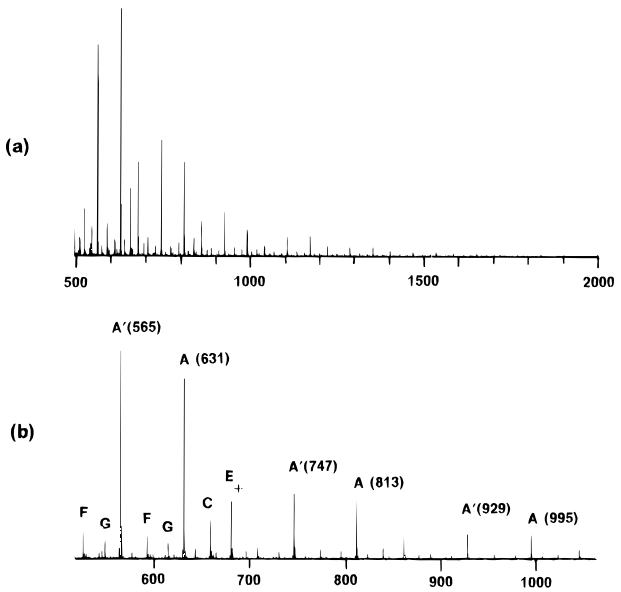

Figure 4. (a) Negative ion TOF-SIMS spectrum of PFP(dioxolane) shown in a linear scale for the 500−2000 amu range. (b) A section of (a) encompassing three successive repeat packets.

attributed to two possible anions resulting from dissociative electron capture at an ether oxygen of Demnum-S. The 50 amu difference between the two peaks is the difference in the mass of the perfluoropropyl and perfluoroethyl end groups at the opposite ends of the chain. We shall designate this type of fragments as type A fragments, and here more specifically as A_p and A_e.

$$CF_3CF_2CF_2O(CF_2CF_2CF_2O)_n^- \qquad MW(A_p) = n(166) + 185$$

$$CF_3CF_2O(CF_2CF_2CF_2O)_n^- \qquad MW(A_e) = n(166) + 135$$

These peaks have nearly identical intensities, reflecting the local symmetry at the ether oxygens.

An essentially identical pattern has been reported previously in an experiment in which Demnum-S was desorbed from a metal surface with one laser, while a second laser was applied to generate low-energy photoelectrons from the metal substrate, and the resulting ions were examined by an ion cyclotron mass spectrometer.[21] The similarity of the cited pattern to that presently observed strongly supports the contention that the negative ion TOF-SIMS spectra of PFPEs are dominated by anions produced by dissociative capture of low-energy electrons.

In addition to type A signals, several additional minor peaks (labeled B, C, and E_-) are observed in each repeat packet (Figure 3b). Some of these signals are due to anions resulting from secondary dissociative electron capture, while others are ascribed to type A signals from polymer chains having impurity constituents. They are discussed collectively in a later section.

PFP(dioxolane). Figure 4a shows, in a linear scale, the negative ion TOF-SIMS spectrum of PFP(dioxolane) in the 500−2000 amu range. Figure 4b shows, in an expanded scale, a portion encompassing three repetitive packets of the pattern. In PFP(dioxolane) ether oxygens are asymmetric. If, on capture of an electron, the bond between oxygen and ethylene unit is preferentially cleaved, the following type A anions are expected.

$CF_3O(CF_2OCF_2CF_2O)_nCF_2O^-$ MW(A) = $n(182) + 151$

$CF_3O(CF_2CF_2OCF_2O)_n^-$ MW(A′) = $n(182) + 85$

If, on the other hand, the bond between oxygen and the methylene unit is preferentially cleaved, the following type A anions are expected.

$CF_3O(CF_2OCF_2CF_2O)_n^-$ MW(A) = $n(182) + 85$

$CF_3O(CF_2CF_2OCF_2O)_{n-1}CF_2CF_2O^-$ MW(A′) = $n(182) + 19$

The observed anion pattern (Figure 4b) reveals that the dissociation occurs exclusively at the bond between oxygen and methylene unit. We rationalize that the proximity of the adjacent ether oxygen (with its negative charge) on the methylene side dictates the dissociation at the methylene side.

Krytox. Figure 5a shows, in a linear scale, the negative ion TOF-SIMS spectrum obtained from Krytox (in the 500−2000 amu range). Figure 5b shows, in an expanded scale, a portion encompassing three repetitive packets of the pattern. Krytox is an isomer of Demnum; its negative ion spectrum is expected to be similar to that of Demnum. However, unlike Demnum, the ether oxygens of Krytox are asymmetric. The relative intensities of the major peaks A_p and A_e may hence be skewed by unequal probabilities.

$CF_3CF_2CF_2O[CF(CF_3)CF_2O]_n^-$ MW(A_p) = $n(166) + 185$

$CF_3CF_2O[CF_2CF(CF_3)O]_n^-$ MW(A_e) = $n(166) + 135$

The observed pattern (Figure 5b) reveals that the O−CF(CF_3) bond is cleaved several times preferentially over the O−CF_2 bond. The observed preference is attributed to the difference in the atomic charges of the ether bound carbons induced by their substituents. Thus, in the absence of an adjacent ether oxygen at the nearest possible position (as with a methylene unit), the dissociative electron capture at an asymmetric ether, R−O−R′ + e^- → R−O^- + •R′, favors the cleavage in which the carbon with more electronegative substituents retain the negatively charged ether oxygen.

Fomblin-Z. Figure 6a shows the negative ion TOF-SIMS spectrum observed from Fomblin-Z (in the 500−1200 amu range). Fomblin-Z consisting of methylene and ethylene oxide repeat units may be thought to have the same constituents as PFP(dioxolane). The difference between the negative ion spectra of these PFPEs (Figure 6a vs Figure 4b) is intriguing. The extraordinary complexity of the Fomblin-Z spectrum is attributed to the random distribution of the repeat units.

The anion spectrum of Fomblin-Z may be simulated based on the following assumptions: (1) The linear sequencing of monomer units in each chain is completely random. (2) The relative amounts of methylene and ethylene units in each chain is that determined by a ^{19}F NMR analysis. (3) The dissociative electron capture occurs at any ether oxygen with equal probability. (4) When it occurs at an asymmetric ether oxygen, the bond between oxygen and methylene unit is cleaved. (5) The weighting factor of a negative ion fragment, $CF_3O(CF_2CF_2O)_m(CF_2O)_n^-$, is then given by its permutation factor $(m + n)!/(m!n!)$. (6) Finally, taking cognizance of

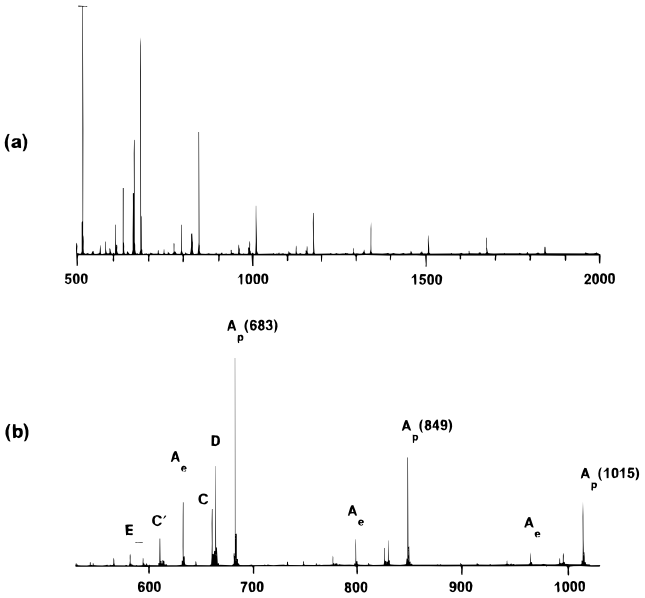

Figure 5. (a) Negative ion TOF-SIMS spectrum of Krytox shown in a linear scale for the 500−2000 amu range. (b) A section of (a) encompassing three successive repeat packets.

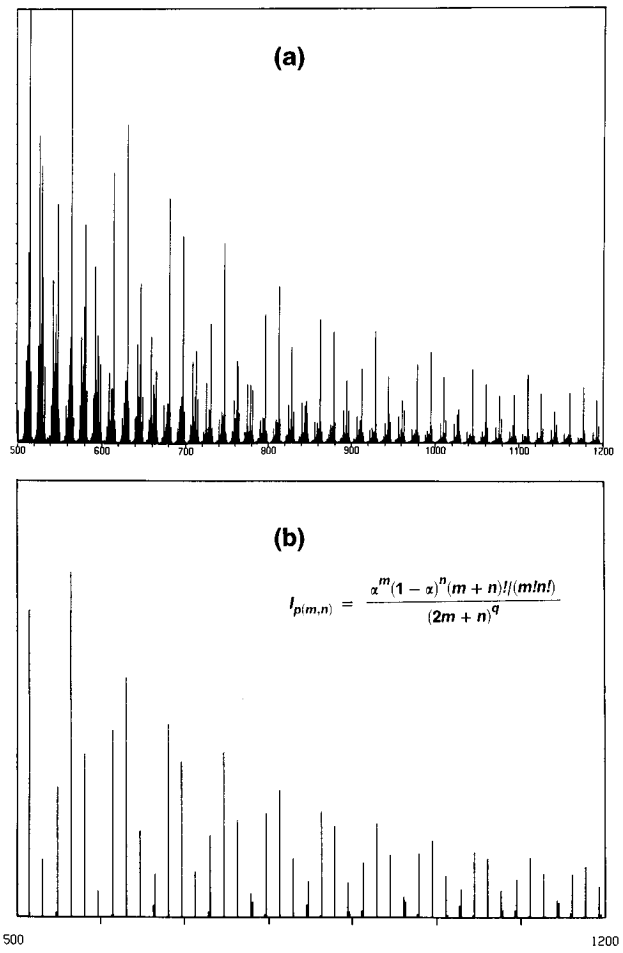

Figure 6. 6. (a) Negative ion TOF-SIMS spectrum of Fomblin Z in the 500−1200 amu range (in a linear scale). (b) A computed intensity pattern of type A anions, $CF_3O(CF_2CF_2O)_m(CF_2O)_n^-$, expected from Fomblin Z. α and 1 − α are the fractional compositions of the ethylene and methylene units (determined by ^{19}F NMR). See text for details.

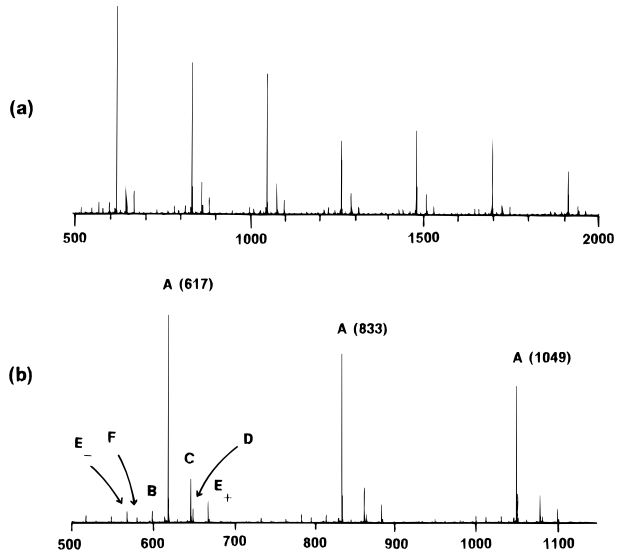

Figure 7. (a) Negative ion TOF-SIMS spectrum of PFP-(tetramethylene oxide) shown in a linear scale for the 500−2000 amu range. (b) A section of (a) encompassing three successive repeat packets.

the fact that the longer the chain, the larger its probability to undergo multiple ionization/fragmentation processes, the overall pattern is damped by a damping factor $(2m + n)^q$.

Figure 6b shows the spectrum simulated for [ethylene unit]/[methylene unit] = 0.48/0.52, and the damping exponential parameter of $q = 2$ (chosen for the best fit). The agreement between the observed and simulated patterns is gratifying.

PFP(tetramethylene oxide). Figure 7a shows, in a linear scale, the negative ion TOF-SIMS spectrum observed from PFP(tetramethylene oxide) in the 500−2000 amu range. Figure 7b shows, in an expanded scale, a portion encompassing three repetitive packets of the pattern. There is only one ether oxygen in each repeat unit, and, as these particular PFP(tetramethylene oxide) chains are terminated with propyl groups at both ends, only one type A signal is expected in each repeat packet.

$$CF_3CF_2CF_2O(CF_2CF_2CF_2CF_2O)_n^- \qquad MW(A) = n(216) + 185$$

Type A peaks are indicatd in Figure 7b.

PFP(ethylene oxide). Figure 8a shows, in a linear scale, the negative ion TOF-SIMS spectrum observed from PFP(ethylene oxide) in the 500−2000 amu range. Figure 8b shows, in an expanded scale, a portion encompassing three repetitive packets of the pattern. Again, there is only one ether oxygen in each repeat unit, and as the polymer chains are terminated with methyl groups at both ends, only one type A signal is expected in each repeat packet.

$$CF_3O(CF_2CF_2O)_n^- \qquad MW(A) = n(116) + 85$$

Type A peaks are indicated in Figure 8b.

Minor Peaks Due to Secondary Electron Capture. The propensity of PFPE molecules to generate anions via dissociative electron capture has thus been demonstrated. It is likely that some of the neutral radicals simultaneously generated by the process are sufficiently stable and thus undergo second dissociative electron capture and generate secondary anions. As

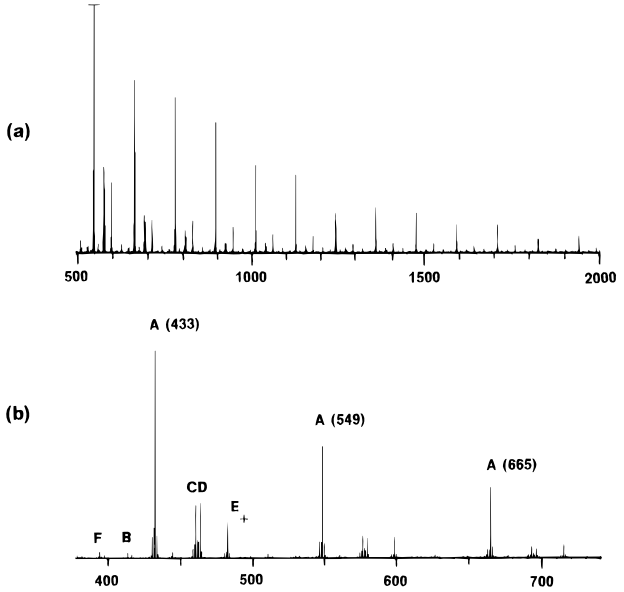

Figure 8. (a) Negative ion TOF-SIMS spectrum of PFP-(ethylene oxide) shown in a linear scale for the 500−2000 amu range. (b) A section of (a) encompassing three successive repeat packets.

stated earlier, the most probable dissociative capture expected for PFPEs is that yielding F^- ions, $R{-}F + e^- \rightarrow R^\bullet + F^-$. Two structural types, I and II, are possible for the neutral radicals $R^\bullet$ thus generated. For Demnum-S, they may be written as follows.

Type I $\quad ROCF_2\dot{C}FCF_2OR'$

Type II $\quad RO\dot{C}FCF_2CF_2OR'$

In type I, the radical center is a bona fide secondary radical (i.e., dialkyl-substituted form). In type II, the radical center is bound to an ether oxygen. We shall designate as type B anions the anion fragments expected to emerge if these neutral radicals undergo the dissociative electron capture at an ether oxygen. It follows that

$$MW(B) = MW(A) - 19 \text{ amu}$$

Minor signals that would correspond to type B anions are indeed recognized for Demnum-S (Figure 3b) and PFP(tetramethylene oxide) (Figure 7b).

Most intriguingly, type B signals are essentially absent in the spectra of PFP(dioxolane) and PFP-(ethylene oxide). We note that, for these polymers, only type II neutral radicals are possible. We envisage that type II neutral radicals undergo spontaneously the following dissociation reaction and yield new polymer chains terminated with an acyl fluoride group.

$$RO\dot{C}FCF_2CF_2OR' \rightarrow R^\bullet + O{=}CFCF_2CF_2OR'$$

If these new chains undergo the dissociative electron capture at an ether oxygen, anions with an acylfluoride end group would be formed. We designate these as type C anions. The following can be readily shown.

for Demnum-S and Krytox: $MW(C) = MW(A_p) - 22$ amu

for PFP(dioxolane), -(tetramethylene oxide), and -(ethylene oxide): $MW(C) = MW(A) + 28$ amu

Signals corresponding to type C signals are clearly observed as indicated (Figures 3b, 4b, 5b, 7b, and 8b).

For PFP(dioxolane), radical ROĊFOR is formed on loss of F^- from a methylene unit; it would dissociate to yield chains terminated with a fluoroformate group.

$$ROĊFOR' \rightarrow R^\bullet + O{=}CFOR'$$

No signals corresponding to anions expected from this type of polymers are observed (Figure 4b). It has been shown that the fluoroformate end group in PFPE is unstable and changes to an acyl fluoride end group as follows.[22]

$$O{=}CFOCF_2CF_2R \rightarrow O{=}CF_2 + O{=}CFCF_2R$$

Neutral radicals R• resulting from dissociative electron capture at an ether oxygen, $R{-}O{-}R + e^- \rightarrow R{-}O^- + {}^\bullet R$, may also undergo the second electron capture, and the resulting *secondary anions* may have the radical end. We designate such anions with a radical end as type D anions. It can be shown readily:

for Demnum-S and Krytox: $MW(D) = MW(A_p) - 19$ amu

for PFP(dioxolane): $MW(D) = MW(A') - 19$ amu

for PFP(tetramethylene oxide) and PFP(ethylene oxide): $MW(D) = MW(A) + 31$ amu

Excepting Krytox, for all the PFPEs examined here the subject radicals R• are primary radicals. Their lifetime should be short; the probability of detecting type D anions should thus be small. Weak D signals are recognized for PFP(tetramethylene oxide) and PFP(ethylene oxide) as indicated (Figures 7b and 8b), but none for PFP(dioxolane). For Demnum-S, peak D coincides with peak B_p. In Figure 3b, we note that, within each repeat packet, B_p is slightly larger than B_e. The difference is attributed to the contribution from type D anions.

For Krytox, the radical end of type D anions would predominantly be a secondary radical (i.e., $CF_3ĊFCF_2OR$). The presence of unusually intense D peaks (Figure 5b) is attributed to the extra stability of secondary radicals. Also noted for Krytox is the presence of peak C′ at 22 amu below peak A_e. Type C anions with the acyl fluoride end group, $O{=}CFCF_2O^-$, would account for this peak. We suggest that the pendant methyl groups of Krytox are particularly prone to dissociate during ionized state, and the following sequence of dissociation occurs.

$$[ROCF(CF_3)CF_2OR']^+ \rightarrow ROĊFCF_2OR' + CF_3^+$$
$$\downarrow$$
$$R^\bullet + O{=}CFCF_2OR'$$

An extra strong signal at 69 amu (CF_3) was observed in the positive ion TOF-SIMS spectrum of Krytox.

Minor Peaks Due to Anomalous Constituents. In addition to minor peaks of type B, C, and D, several additional minor peaks are seen within each repetitive packet of the negative ion spectra (Figures 3b, 4b, 5b, 7b, and 8b). These signals are attributed to type A signals resulting from parent molecules vested with anomalous end groups and/or intrachain monomer units. Most of these peaks are positioned at either (1) 50 or 100 amu above or below the associated A peak or (2) 38 amu below the associated A peak. An end group or an intrachain unit having one or two additional (or less) CF_2 unit(s) would account for the former class of signals. An end group or an intrachain unit having a double-bond sector $-CF{=}CF-$ would account for the latter.

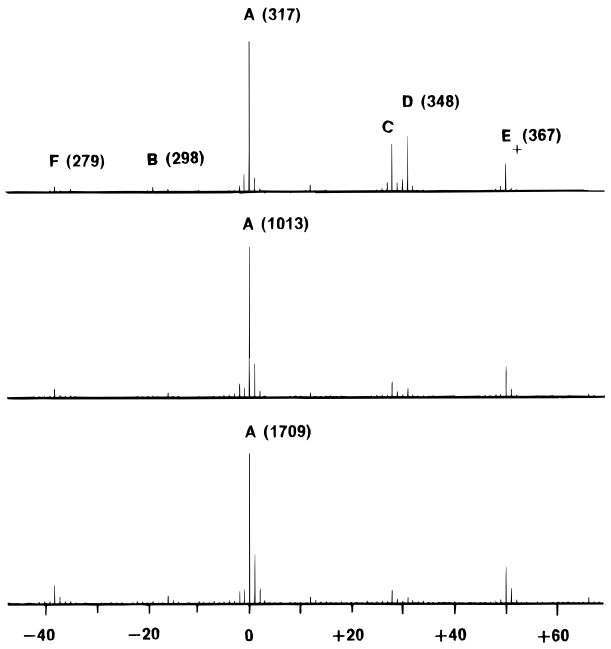

Figure 9. Negative ion TOF-SIMS spectrum of PFP(ethylene oxide). Three widely separated repeat packets are shown atop each other so that horizontal positions of the same type of signals coincide. The scale is normalized against peak A in each packet. The three A peaks are due to $CF_3O(CF_2CF_2O)_n^-$, where n = 2, 8, and 14.

The ^{19}F NMR spectra of these polymers revealed the presence of a small fraction (~3%) of methyl end groups in Demnum-S, a substantial fraction (10−20%) of ethyl end groups in PFP(dioxolane) and PFP(ethylene oxide), and some fraction (~10%) of butyl end groups in PFP(tetramethylene oxide). If the anomalous component is in the end group, the intensity of the subject minor peak relative to the A peak in the same repetitive packet is expected to remain constant from one packet to another. If, on the other hand, the anomalous component is in a intrachain unit, the relative intensity of the minor peak is expected to increase as the number of repetitive units in the negative ion increases.

Figure 9 shows, in an expanded scale, three separate sectors of the negative ion spectrum of PFP(ethylene oxide). Three packets are shown atop each other so that the positions of the same type of signals coincide. The vertical scale is normalized against peak A in each packet. The three A peaks thus shown are $CF_3O(CF_2CF_2O)_n^-$, where n = 2, 8, and 14, respectively. We note immediately that the intensities (relative to A) of minor peaks due to secondary electron capture, B, C and D, diminish rapidly with increasing chain length. This is attributed to the radical state, hence the shorter lifetime, of the precursors of these secondary species. The probability of such radicals to fragment or to undergo intramolecular reaction would increase with increasing chain length. In the case of type D anions, the mass distribution of the precursor radicals R• must be similar to that given by type A anions.

In contrast to the intensities of the secondary species, the intensity of the peak at 50 amu above peak A remains constant. These peaks are thus assigned to type A signals resulting from parent chains having an end group with an extra CF_2 unit. We shall label these

signals as E_+. In further contrast, the intensity of the peak at 38 amu below its associated A peak increases with increasing chain length. These peaks are thus assigned to type A signals resulting from parent molecules contaminated with an intrachain unsaturated unit $-CF{=}CF-$. These signals are labeled as type F. Similar intensity analyses were made for other PFPEs, and essentially all the minor peaks extraneous to B, C and D types were assigned as either type $E_\pm$ or F (Figures 3b, 4b, 5b, 7b, and 8b). PFP(dioxolane) shows additional minor signals at 16 amu below A and A′ (labeled G in Figure 4b). Based on the mass difference and the intensity variation, type G signals were attributed to anomalous intrachain units $CF_2CF_2CF_2O$.

Summary and Concluding Remarks

The present study has revealed the following.

(1) Negative ion TOF-SIMS spectra of PFPEs have intense, simple patterns persisting into the high-mass region, surpassing the mean MW of the sample polymers.

(2) The negative ion yield in this range (>200 amu) is 2 orders of magnitude larger than that of positive ions.

(3) All the major peaks in the persistent negative ion pattern are ascribable to anions generated by one-step dissociative election capture at ether oxygens.

(4) For locally asymmetric ether oxygen, preferential dissociative capture at one C−O bond over the other occurs in a readily rationalizable fashion.

(5) The intensity of signals due to secondary processes, dissociative electron capture by neutral radicals generated in the primary event, is diminishingly small above 1000 amu.

A negative ion TOF-SIMS study of PFPE is thus an extremely sensitive and useful route to elucidate structural features of parent PFPE chains. Recently, it was shown that PFPEs have a propensity to undergo the *intramolecular disproportionation* of the following scheme.[23]

$$RCF_2OCF_2R' \rightarrow RCF_3 + O{=}CFR'$$

Fragmentation of PFPEs, and formation of organic debris containing carboxylic groups at the head−disk interface of magnetic recording systems have been reported by several authors.[24,25] A TOF-SIMS study of PFPEs applied on magnetic recording disks, and their metamorphoses under tribological condition is an obvious extension of the present study.

References and Notes

(1) Moulder, J. F.; Hammond, J. S.; Smith, K. L. *Appl. Surf. Sci.* **1986**, *25*, 446.
(2) Snyder, C. E.; Gschwender, L. J.; Campbell, W. B. *Lubr. Eng.* **1982**, *38*, 41.
(3) Clampelli, F.; Venturi, M. T.; Sianesi, D. *Org. Magn. Reson.* **1969**, *1*, 281.
(4) Briggs, D. *Surf. Interface Anal.* **1982**, *4*, 151.
(5) Benninghoven, A.; Colton, R. J.; Simons, D. S.; Werner, H. W. *Secondary Ion Mass Spectrometry V*; Springer-Verlag: Berlin, 1986.
(6) Hues, S. M.; Colton, R. J.; Mowry, R. L.; McGrath, K. J.; Wyatt, J. R. *Appl. Surf. Sci.* **1988**, *35*, 507.
(7) Hues, S. M.; Wyatt, R. R.; Colton, R. J.; Black, B. H. *Anal. Chem.* **1990**, *62*, 1074.
(8) Bletsos, I. V.; Hercules, D. M.; Fowler, D.; vanLeyen, D.; Benninghoven, A. *Anal. Chem.* **1990**, *62*, 1275.
(9) Newman, J. G.; Viswanathan, K. V. *J. Vac. Sci. Technol.* **1990**, *A8*, 2388.
(10) Viswanathan, K. V. *J. Appl. Polym. Sci., Appl. Polym. Symp.* **1990**, *45*, 361.
(11) Fowler, D. E.; Johnson, R. D.; vanLeyen, D.; Benninghoven, A. *Surf. Interface Anal.* **1991**, *17*, 125.
(12) John, C. M.; Radicati di Brozolo, R.; Odom, R. W.; Shingu, K.; Yoshino, N.; Amemiya, T. In *Secondary Ion Mass Spectrometry IX*; Benninghoven, A., Nikei, Y., Shimizu, R., Werner, H. W., Eds.; John Wiley and Sons: New York, 1994.
(13) Feld, H.; Leute, A.; Rading, D.; Benninghoven, A.; Chiarelli, M. P.; Hercules, D. *Anal. Chem.* **1993**, *65*, 1947.
(14) See, for example: Willson, C. G. In *Introduction to Microlithography*; Thompson, L. F., Willson, C. G., Bowden, M. J., Eds.; American Chemical Society: Washington, DC, 1983; pp 122−140.
(15) See, for example: Märk, T. D. In *Electron−Molecule Interactions and Their Applications*; Christophorou, L. G., Ed.; Academic Press, Inc.: London, 1984; pp 251−334.
(16) Kasai, P. H. *J. Am. Chem. Soc.* **1990**, *112*, 4313.
(17) Kasai, P. H. *J. Am. Chem. Soc.* **1991**, *113*, 3317.
(18) Schueler, B.; Sander, P.; Reed, D. A. *Vacuum* **1990**, *41*, 1661.
(19) Schueler, B. *Microsc. Microanal. Microstruct.* **1992**, *3*, 1.
(20) Briggs, D.; Hearn, M. J. *Vacuum* **1986**, *36*, 1005.
(21) Cromwell, E. F.; Reihs, K.; deVries, M. S.; Ghaderi, S.; Wendt, H. R.; Hunziker, H. E. *J. Phys. Chem.* **1993**, *97*, 4720.
(22) Sianesi, D.; Pasetti, A.; Fontanelli, R.; Bernardi, G. C.; Caporiccio, G. *Chim. Ind.* **1973**, *55*, 208.
(23) Kasai, P. H. *Macromolecules* **1992**, *25*, 6791.
(24) Novotony, V. J.; Karis, T. E.; Johnson, N. W. *J. Tribology* **1992**, *114*, 61.
(25) Xuan, J.; Chen, G.; Chao, J. *IEEE Trans. Magn.* **1993**, *29*, 3948.

MA951341D